Study on moderate earthquake risk of the Xinfengjiang reservoir from 3D P-wave velocity structure and current seismicity parameters

Xiuwei Ye*, Xiaona Wang, Yuanmin Huang, Jiping Liu and Zhengguang Tan

Key Laboratory of Earthquake Monitoring and Disaster Mitigation Technology, Guangdong Earthquake Administration, Guangzhou, 510070, China

*Corresponding e-mail: 1424201562@qq.com

Abstract. In this paper, we determined the Xingfengjiang Reservoir earthquake sequence location from June 2007 to July 2014 and 3D P-wave velocity structure by a simultaneous inversion method. On that basis, we mapped the *b*-value 3D distribution. The results show the low *b*-value distribution consists with the high velocity zone(HVZ) and most earthquakes occurred around the HVZ. Under the reservoir dam there is a strong tectonic deformation zone, as the centre exit Renzishi fault F2, Nanshan - Aotou faults F4, Heyuan fault F1 and Shijiao-xingang-baitian fault F5. M6.1 Xinfengjiang earthquake, 19 Mar 1962, occurred in the strong tectonic deformation zone, and now the zone $b \geq 0.7$, so a short period of the original earthquake occur more unlikely. The *b*-value of the HVZ under Xichang(in the northwest corner of XFJ Reservoir) ranges between 0.4 to 0.7 suggesting the rate of stress accumulations is greater than the speed of seismic energy release since 2012. We don't exclude the possibility that the HVZ becomes the seismogenic asperity, and will occur M≥5 earthquake.

1. Introduction

In recent years, XinfengJiang (hereafter referred to XFJ) Reservoir of Guangdong is one of the most active seismic regions in southern China. Seven $M_L \geq 4$ earthquakes has occurred from 2012, in which the most devastating one with a magnitude of 4.8 occurred in Xichang (in the northwest corner of XFJ Reservoir) on 16th February 2012, therefore there is an accentuated concern for XFJ Reservoir region. Seismic activity were focused near the dams of XFJ Reservoir before the M4.8 Xichang earthquake, including the M6.2 earthquake that occurred 1km away from the dam in 1961. In the past, seismic research for the tectonic activities, velocity structure and earthquake hazards were focused on the XFJ Reservoir dam and the centralised Reservoir [3, 5-8, 18, 26, 27]. While with the northwest expansion of seismic activity there is an outburst of 4-5 moderate earthquakes happened surrounding Xichang. Thus seismic research is significant for these gradually maturing conditions neighbouring XFJ Reservoir.

"Earthquake forecast using earthquake" is still the primary method to study seismic hazards, and accurate relocation of the earthquake sequence is elementary for reliable results. With today's technology, using the high-definition crust velocity model is the one of the most accurate and effective way. With the development of seismic tomography technology [1, 14, 24, 46]; the construction of 3D velocity structural models provides the basis of seismic location. Jointly inversion of source parameters and velocity structure [4, 11, 12, 17, 20, 23, 51] can obtain improved location accuracy as well as structural velocity. By applying this method, earthquake sequences have been resolved successfully in our country. [13, 16, 19, 45, 52, 53]. This paper will use this method to obtain relatively accurate spatial distribution of earthquake sequence and 3D P-wave velocity structure of the upper crust in XFJ Reservoir. On this basis, we will carry on the 3D *b*-value scanning process.

Experimental investigation of rock failure [21], seismic activities research about rock fractures and fluid extractions as well as mine rock rupture observations [25] etc. indicates that the stress is inversely proportional to the *b*-value in the G-R relation between the earthquake magnitude(M) and frequency (N) [9].

$$\lg N = a - bM \tag{1}$$

The lower the *b*-value the higher the stress level. a, b in fomula (1) are regression constants. As a major parameter for estimating the fault zone relation with its stress level in seismic activity, The *b*-value has been widely used in long-term seismic hazards assessment [15, 22, 29-32, 36-38, 40-42, 48]. In this paper, we undertake the *b*-value 3D scans using the re-justified sequential listings, then discuss the future seismic hazards combining regional tectonic and velocity structure in XFJ Reservoir. The future seismic hazards will serve as a precedent and provides strong structural reference the whole eastern region.

2. Method

In the joint inversion process of the source parameters and velocity structure [12, 16, 52], its travel time residualδt is caused by the disturbances of source and speed parameters, For l earthquakes and j stations., they can be expressed in the following formula:

$$\delta t = A\delta v + B\delta x \tag{2}$$

In this formula, δt(M×1) is the travel time residual vector, δv(N×1) is the node velocity perturbation vector and δx(4l×1) is the source parameters perturbation vector. Also, A(M×N) is partial derivative of the source parameters of the travel time matrix. Since the velocity parameter and its source parameter are mutually coupled in equation (2), if we simultaneously inverse 2 different dimensional parameters in the source equation, it will increase the numerical instability in the algorithm as well as consuming a large amount of computer resource. In this case, it must be a separate argument. In this paper, by using Liu Futian's [12] orthogonal projection, formula (2) can be divided into the following 2 equations to find its velocity parameter and source parameters:

$$(I - P_B)A\delta v = (I - P_B)\delta t \tag{3}$$

$$B\delta x = P_B(\delta t - A\delta v) \tag{4}$$

Within the equation, P_B is the orthogonal projection operator from the R^m to image space $R(B)$ of B related to the source parameters. The analysis indicates that there is no direct relationship between the velocity and source perturbation after developing the velocity and source parameters. It is clear that the velocity and source perturbation is significantly related to its initial value only. According to equations (3) and (4), in the joint inversion process, it is important to determine the velocity structure parameter first, than determine the source parameter regarding to the study area. This will eliminate the impact of any uncertainties related to the velocity structure as well as helping to position its accuracy. Therefore, through joint inversion of the source parameter and velocity structure, it can effectively improve the accuracy of the earthquake location and obtain the velocity structural model within the inversion.

The b-value 3 dimensioanl scanner is used from Wiemer S. University of Washington and Zmap program [33], in determining the minimum integrity of the magnitude and is the most likely method used for scanning.

3. Data and model

3.1. Earthquake data processing and velocity model building

The digital seismic network had been running since June 2007. In this paper, we calculate the inversed velocity structure (figure 1) by using 91,666 P-wave travel time of 13,247 earthquakes recorded from June 2007 to July 2014 to. XFJ Reservoir is the most active seismic region of Guangdong province; its digital seismic network composes of five seismic stations. After Xichang M4.8 earthquakes in 2012, three more portable seismic stations were set to increase observations and to make more complete sequence records.

According to the ray path distribution map (figure 2), the study area (114.4°-114.8°E, 23.2°-24.4°N) has high internal ray density, whereas border areas has slightly lower ray densities. Therefore, The area with high internal ray density have a spacing of 0.03° to 0.05°, while border areas have a spacing of 0.1° to 0.4° (figure2).

Detailed documentation of the initial velocity structure inversion model: Ye Xiuwei，2013；Zheng Qisen，2003；2004； Geology and mineral resources Bureau of Jiangxi province，1984；Wen Zegang，2005；Yao Bochu，1994；Xu Huilong，2006；Zhao Minghui，2004.

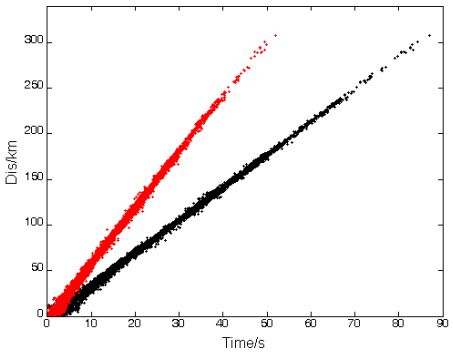

Figure 1: P wave and S wave's travel time

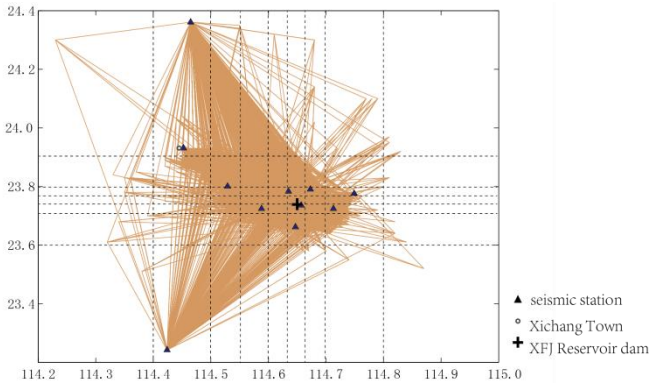

Figure 2: Ray path distribution and model grid

3.2. Resolution analysis

In this paper, we use checkboard resolution test to estimate and explain the reliability of the resolution. The results show (figure 3), the resolusion from XFJ Reservoir Dam to the northwest corner Xichang is acceptable above 15km in the upper crust due to its relative high earthquake frequency and station density.

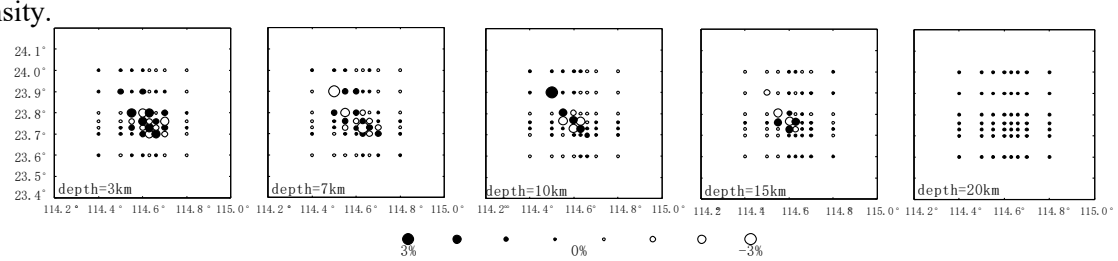

Figure 3: Checkboard resolution test in 3km, 7km, 10km, 15km, 20km depth

3.3. b-value scans parameters

For the earthquake ML≥0.3, the magnitude– frequency linear fitting correlation coefficient R= -0.994, the slope b= 0.9042, taking a minimum magnitude of completeness Mc= 0.3(figure 4). We determine the end location of the cross-section according to the earthquake and its structural distribution. Then we calculated the b-value with the maximum likelihood calculation method by using at least 30 earthquakes within 5km of the cross-section, moreover, the grid spacing is 0.5×0.5km and the structural unit radius r is 5km. Finally we draw a cross section image based on the distribution of the b–value nodes.

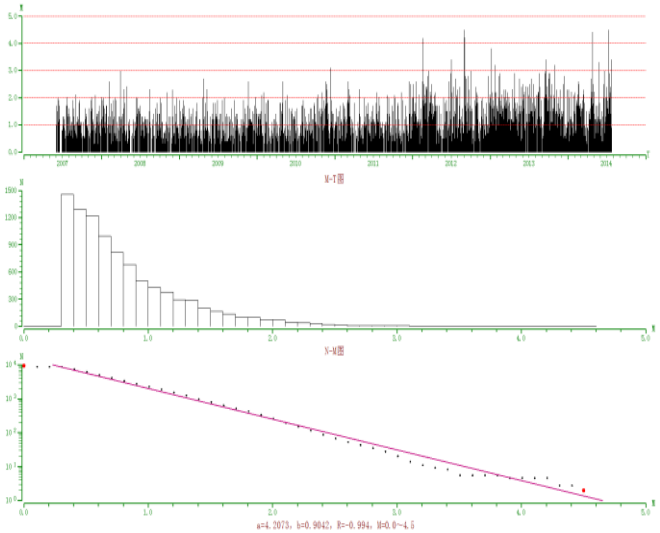

Figure 4. M-T and Magnitude-frequency curve in XFJ Reservoir

4. Result calculations

To more directly reflect the P value velocity structure and the b-value distribution of XFJ Reservoir, we provided a plan with several groups of typical b-value profiles and a P- wave velocity chart. The profiles included: the east-west AB and the north-south GH cross sections through Xichang; the NW-SE EF cross section across the entire reservoir area and the IJ cross section parallel to EF sectional profile (Figure 5). The general plan and profile images shown as follows.

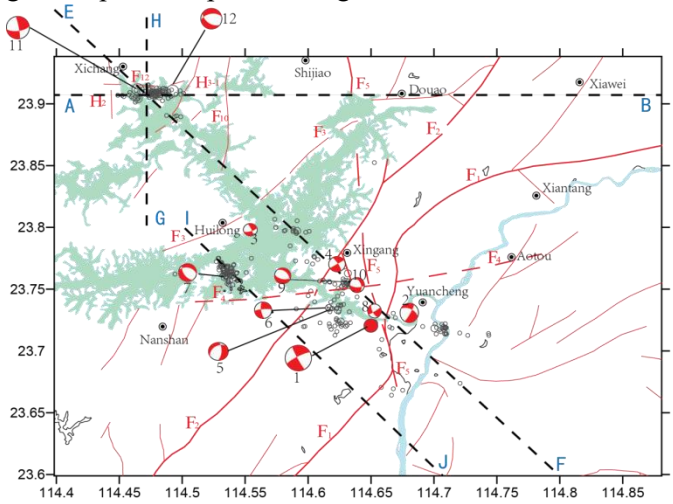

Note: (From 2007.06 to 2014.07 $M_L \geq 1.5$ and Focal mechanism solutions of 12 events)
F1: Heyuan Fault; *F2:* Renzishi Fault; *F3:* Daping-Yanqian Fault; *F4:* Nanshan-Autou Fault; *F5:* Shijiao-Xingang-Baitian Fault; *F10:* Lanwu-Taihedong Fault; *F12:* Dakengnan inferred Fault; *H2:* Xichang Syncline; *H3-1:* Wushimen-Yutan Fold group (similarly hereinafter)
1 1962-03-19M6.1; *2* 1964-09-23M5.1; *3* 1971-02-25M3.5; *4* 1972-12-18M4.1; *5* 1975-07-25M4.3; *6* 1977-05-12M4.2; *7* 1987-09-15M4.7; *8* 1999-03-25M4.2; *9* 1999-08-20M4.7; *10* 2012-08-31M4.0; *11* 2012-02-16M4.8; *12* 2013-02-16M4.7
(Focal mechanism solutions No.1-9 came from Wei Bolin(2001); No.10-12 came from Yang Xuan)

Figure 5: earthquake epicentre distribution, structure and section lines in XFJ Reservoir

4.1. P-wave velocity and b-value plan distribution diagram

From the results of the sectional plan of XFJ Reservoir, the focal depth is concentrated to 5-15km. The depth of high velocity body in the upper crust locates within 6-12km (later in this article for an expanded discussion of this topic), therefore the selected depth of 8km of the P- wave velocity is a relatively reliable representation (figure 6a). The figure shows that the high velocity areas spread southeastward from Xichang to the vicinity of the XFJ reservoir dam, which having a relative consistent distribution with low b-value areas (Figure 6b). XFJ's seismic activity became vigorous after 2012. A series of moderate earthquakes and micro-seismic group activities occurred near Xichang, Huilong and the resevior dam. In comparison to b-value before the 4.8 earthquake in Xichang on 16th Feb 2012, the b-value of Huilong and Xichang has decline (Figure 6c).

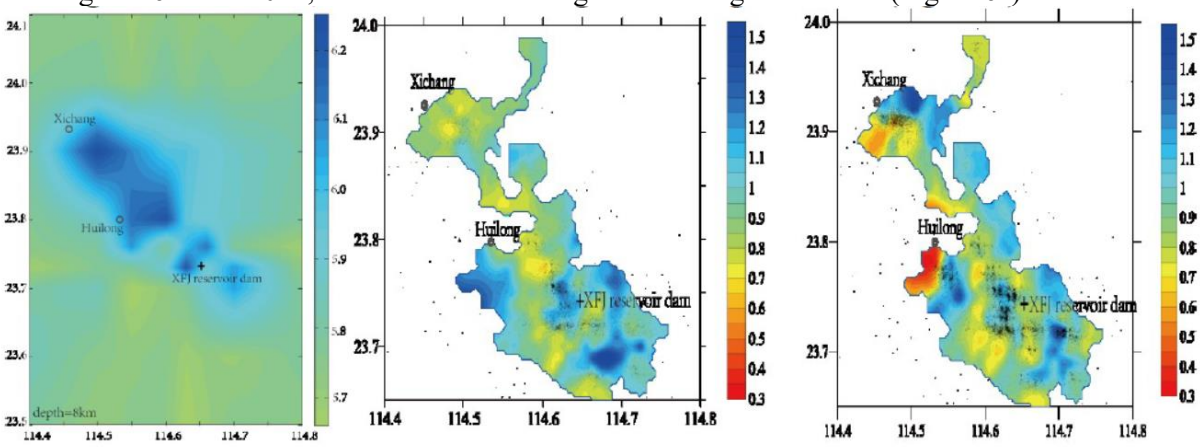

(a) P-wave velocity(depth=8km) (b) *b-value* (2007.06.01-2012.02.15) (c)*b-value* (2007.06.01-2014.07.31)

Figure 6. distribution of P-wave velocity, *b-value* and earthquakes ($M_L \geq 0.3$)

4.2. AB(N23.9°A) and GH(E114.47°) Cross section

AB, GH sections are EW profile and NS profile near Xichang respectively. Summarising from the AB velocity profile (Figure 7a)，the Xichang syncline (H2) has a tendency towards the East, with a depth of more than 15km, its inclination is relative greater in shallow parts and gradually yielded after 13km. The depth of 8-12km in East wall has approximately 6 ×7km high velocity body with the central velocity of up to 6.3km/sec. Since 2012, Xichang's seismic activities mainly concentrated in the west segment of the high velocity body east of H2. Lanwu- Taihe fault F10 also has a tendency towards the east, its high velocity body locates between the south -north faults(H2 and F10) . GH section (Figure 8a) shows that concentrated seismic activities are distributed at the depth of 5-14km, the earthquakes' surface projections are consistent with the strike and location of inferred F12 fault (Figure 5). The GH gross section deduce F12 fault dip to south with a 80° inclination angle.

Before the 4.8 earthquake on 16 February 2012, areas with low b-values mainly located in the west segment of high velocity body (Figure 7c), the low b-value area is roughly consistent with the high velocity body, which indicating high velocity areas are high stress areas. the rupture process of 4.8 earthquake happens from top to bottom, the initial rupture locate above the west top edge of the high velocity body [45], where the b-value ≤0.7 area. Since 2012, there are a continuous of moderate earthquakes (with the magnitude of 4.8, 4.7, 4.2) happening. the seismic activities mainly concentrate in the west of low b-values area with high velocity. The current regional stress levels have not declined, but the Δb image (Figure 7d) shows that the b-value has declined from the middle part of high velocity body, low b-values are trending to expand towards the east.

GH cross section (Figure 8a) shows that, seismic activities mainly concentrat in the inferred south wall and 9 km below north wall of fault F12 from 2012. Also, after the series of moderate earthqukes occurred at Xichang, the b-value has declined ($|\Delta b|_{max} = 0.35$) in the southern footwall.

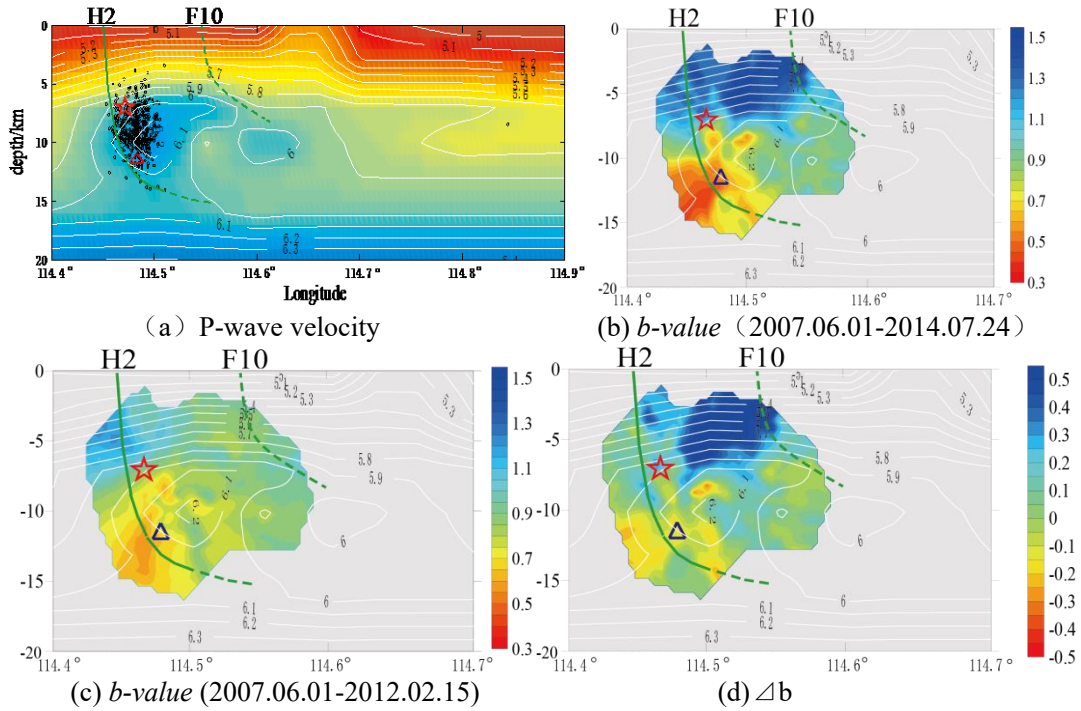

（a）P-wave velocity (b) *b-value*（2007.06.01-2014.07.24）

(c) *b-value* (2007.06.01-2012.02.15) (d) ⊿b

star: M4.8 earthquake on 16 February 2012 triangle: M4.7 earthquake on 22 February 2013

Figure7. AB Cross section of P-wave velocity and b-value（M_L≥1）

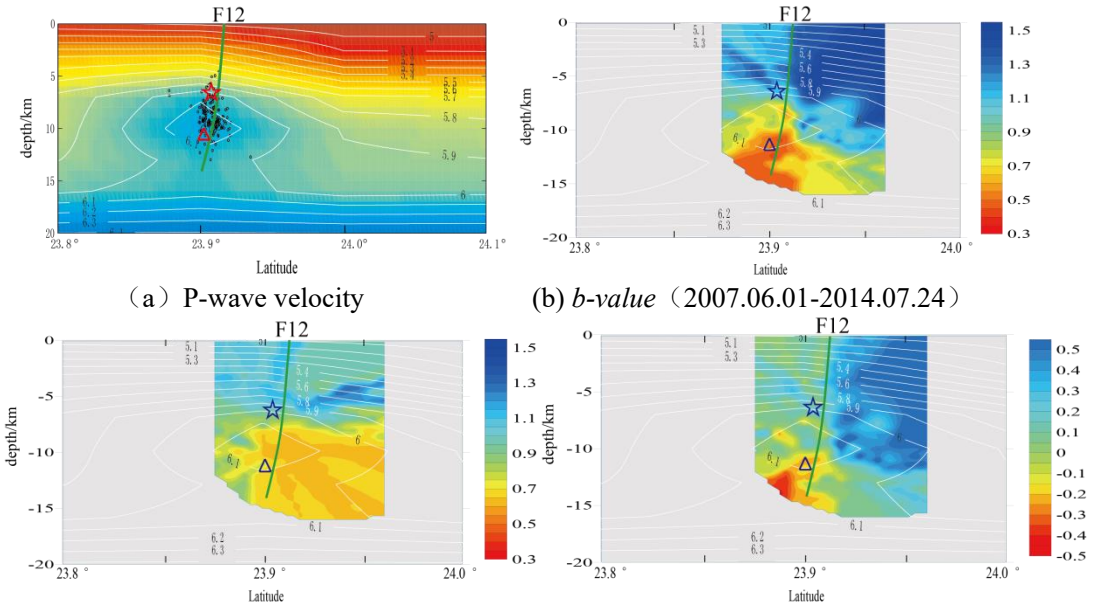

（a）P-wave velocity (b) *b-value*（2007.06.01-2014.07.24）

(c) *b-value* (2007.06.01-2012.02.15) (d) ⊿b

star: M4.8 earthquake on 16 February 2012 triangle: M4.7 earthquake on 22 February 2013

Figure8. GH Cross section of P-wave velocity and b-value（M_L≥1）

4.3. EF and IJ cross section

Deep seismic experiment results of active source [44] and previous studies of our group [45] consistently show that: in the EF cross section, the upper crust from Xichang to the reservoir dam exists a relative high velocity body with speed up to 6.1km/sec, the depth of abnormal body in reservoir dam is 3.5-8.5km with a slightly deeper Eastern ,while the depth of Xichang is up to approximately 10km. With the increase of small earthquakes records, we replace the original

0.1°x0.1° grid to 0.03° ~0.05° grid in the core region between the dam and Xichang. The results (Figure 9a) show that from the dam facing to the Eastern Xichang, 7-14km North West, exist four high velocity bodies. the body I beneath the Xichang has the largest capacity size (approximately 6km x 7km) with the highest velocity and the velocity in the centre is up to 6.3km/s. Followed by body III (approximately 5km x 6km), with speed in the centre up to 60.2km/s. The other two bodies are relative smaller in size and have a central speed of 6.2km/sec and 6.1km/sec respectively. Several faults in the enveloping reservoir distribute further towards the deeper level. Comparing to the previous two EF sectional profile results, this analysis shows a higher resolution.

Figure 9c show that, before the 4.8 earthquake in 2012, the b-value of EF sectional profile shows that the lowest *b*-value(≤0.6) located west of the high velocity I beneath of the Xichang. The lowest *b*-value area occurred M4.8 in 2012, M4.7 in 2013 and a serious of moderate earthquakes in 2014 shortly afterwards.

Figure 9b and 9d shows that, after the earthquake swarm in 2012, regions that have significant decreased b-values cross the EF section are: the centre of high velocity body I beneath the Xichang; the area below high velocity III, and the area above high velocity IV. High velocity body IV had a relative high b-value originally, which is still considered within the normal range although it has decreased by 0.3. The region beneath high speed body III has a low b-value, but it is unlikely that the strain energy will accumulate due to a low velocity. It is worth noting that, as previously indicated in AB and GH sectional graphs, the high velocity I is extending toward south-east the b-value (between 0.4~0.7)have decreased in the centre of the high velocity body, which shows stress energy accumulation.

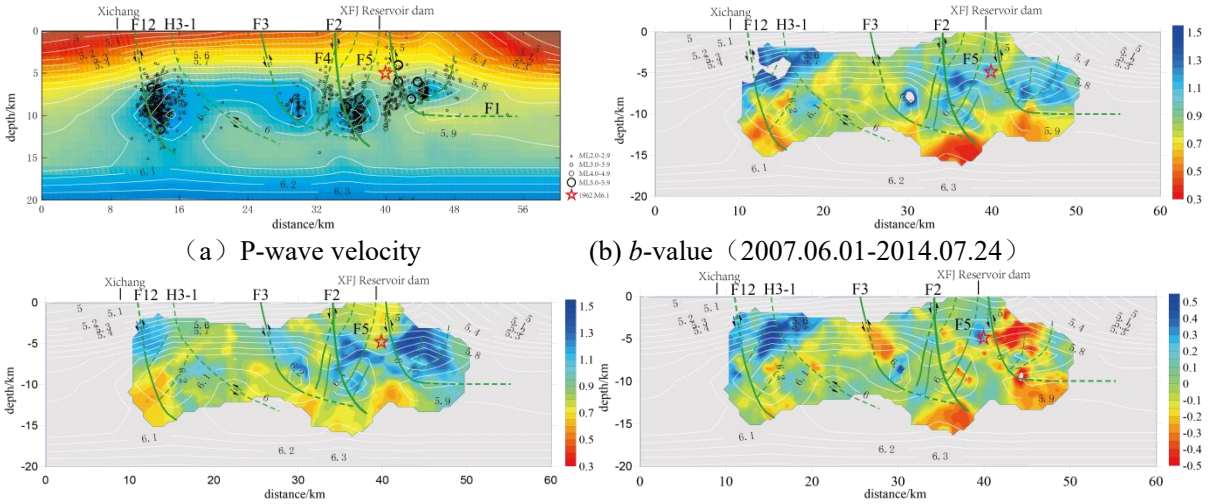

（a）P-wave velocity (b) *b*-value（2007.06.01-2014.07.24）

(c) *b*-value (2007.06.01-2012.02.15) (d) ⊿b

Figure9. GH Cross section of P-wave velocity and *b*-value（M_L≥1）

The IJ cross section is perpendicular to three NE fault lines, including Daping- Yanqian rock fracture F3, Renzishi fault F2 and Heyuan Fault F1. Concluding from figure 10a, Dapings-Yanqian fault dip to southeast with a small angle, which is consistent with the geological data[5]. A seires of seismic activities occurred south of Huilong in September 2013. Small earthquakes occurred along the NW-SE direction (Figure 5). This earthquakes manly occurred on the hanging wall of the fault F3 above the high speed body (Figure 10c). After Donyuan's 4.8 earthquake in 2012, Huilong's b-value has significantly declined (Figure 6C). Section IJ cuts through Huilong's b-value region. Figure 12c shows Donyuan region did not exist observably low b-value region before the 4.8 earthquake, while while the b-value distribute at the 5-10km depth along Daping-Yanqian fault F3 ($|\Delta b|_{max}$= 0.75) decreased most significant in the bottom region of Huilong's earthquake swarm and the lower edge of the north-western of the high velocity body (Figure 9d). which indicates there has been acceleration of strain energy accumulation in high stress areas.

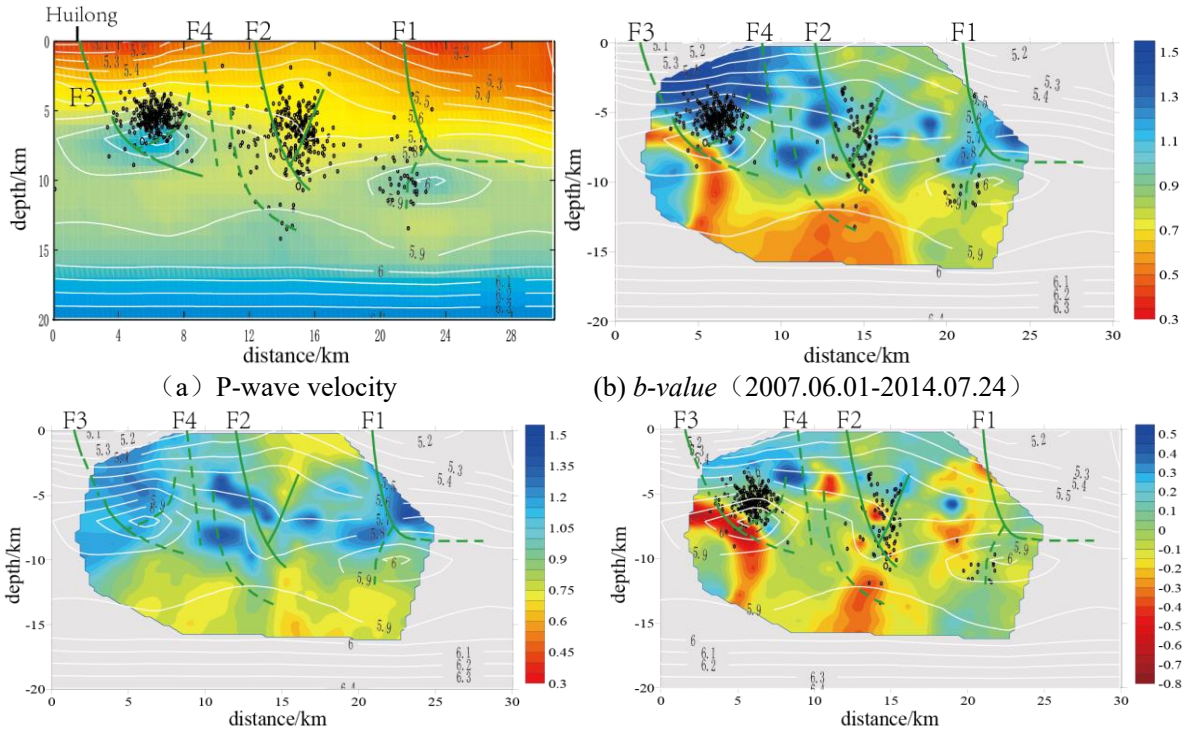

（a）P-wave velocity (b) *b-value*（2007.06.01-2014.07.24）

(c)b-value（2007.06.01-2012.02.15） (d) ⊿b

Figure10. IJ Cross section of P-wave velocity and *b-value*（M_L≥1）

5. Discussions and Conclusions

(1) Comparing XFJ Reservoir P-wave velocity and its b-value scan results, the low b-value region is consistent with its high velocity region. The multi fault lines in the reservoir area envelopes the high velocity body, its ruptures area distributing into deeper depth. Most earthquakes occurred either around, on the edge or through the high velocity body. Clearly, high velocity bodies become the "hot spots" for stress energy accumulation and release on fractured surfaces; it is possible to become seismogenic asperity [2].

(2) Figure 9a cross section reveals that: in the Areas beneath the Dam reservoir where the Renzishi fault F2, Nanshan- AoTou fault F4, Shi Jiao fracture F5 and Heyuan fracture F1 etc staggered distribution, the upper crustal interface on various velocity layers above 7-8km has significant camber deformations , while the deformed velocity layers at the depth 10-15km appears to be concave, which generally reflect intense tectonic deformation zone with F1, F2, F4 and F5 as the centre exist below the dam that there are and area reflected. The deformation zone contains three high velocity bodies, II, III, IV. where occurred 10 M≥5 earthquakes in the instrumental record since 1962, including the 6.1 earthquake. Sectional b-value scans (Figure 9b) show that b≥0.8 in the area of 13km, indicates that the release of stress energy is more complete in the tectonic deformation area, which suggests the possibility of occurrence of earthquakes stronger than 6.0 is unlikely in recent years.

(3) High velocity body located beneath Donyan Xichang area has the largest capacity size (approximately 6km x 7 km) and the highest velocity, with the velocity of 6.3km/sec in the center of the high velocity body . The summary of section b-value scan results from various directions (Figure 7b, 8b) shows: west portion of the high velocity body has a relative low b-value (b≥0.7). Since 2012, many moderate earthquakes have occurred while the b-value in high velocity body's west portion still decrease and has a tendency to expand eastwards and downwards. This simulation. The b-value ranges between 0.4 to 0.7 suggesting the rate of stress accumulations is greater than the speed of seismic energy release since 2012.

(4) After the 6.1 earthquake in 1962, seismic activity in XFJ Reservoir mainly concentrated in areas near the dam, the upstream gorge and central area of the reservoir. Little study was conducted in the

NW corner of the reservoir area. The velocity profile (Figure 7a, 8a) show that the NS trending Xichang syncline (H2) and The inferred EW trending Dakengnan fault F12 have depth reach up to15km. Since the fault is deeper than 15km, and has a lower resolution, two fractures described above needs other methods for validation. After 2012, seismically active area of the reservoir area has a clear migration trend from the SE to NW. In the recent three years, 2 earthquakes with m≥4.5 occurred in the eastern Xichang. With a combination of b-value scan result analysis, we suggests that there may be a high velocity body beneath Xichang become seismogenic asperity, where M>5 earthquakes may occur.

(5) After the series of earthquakes in Xichang in 2012, another series of intense earthquakes activities occurred in Huilong, southeastern Xichang in September 2013. The 3D b-value scan results shows that the b-value at the depth 5-10km along Daping-Yanqian faulthas experienced a significant decrease ($|\Delta b|_{max}= 0.75$) , and the Low b-value areas located in the lower edge of NW of the high velocity body. Taking into account the smaller capacity of the high velocity body, we should note the possibility of moderate earthquakes in the south of Huilong.

Acknowledgement
National Natural Science Foundation of China 41676057.
Thanks to researcher Zhou Longquan in CENC for providing programs of joint inversion calculation with the velocity structure and focal positions . Thanks to researchers Wen Xueze and Yi Guixi in Sichuan Seismological Bureau for providing valuable advices and help about the velocity profile structures and b-value scan results interpretations provided . And finally, thanks to earthquake monitoring centre of Guangdong province for providing high quality seismic phases.

References

[1] Aki K, Lee W H K. 1976. Determination of three-dimensional velocity anomalies under a seismic array using P arrival times from local earthquakes．1．A homogeneous initial model. *J Geophys Res*, (81):4381-4399
[2] Aki K. 1984. Asperities, barriers, characteristic earthquakes and strong motion prediction. *J Geophys Res*, (89):5867-5872
[3] Chen Y M. 1982. The focal mechanism study of Xinfengjiang reservoi-induced earthquakes and its micro aftershocks. *South China Journal of Seismology* (*in Chinese*), **2**(3): 64-71
[4] Crosson R S. 1976. Crustal structure modeling of earthquake data.1.Simultaneous least squares estimation of hypocenter and velocity parameters. *J Geophys Res,* (81):3036-3046
[5] Ding Y Z. 1989. The Reservoir Induced Earthquake (in Chinese). Beijing：Seismological Press
[6] Ding Y Z, Pan J X, Xiao A Y, et al. 1983. Tectonic environment of reservoir induced erathquake in the Xinfengjiang reservoirarea. *Seismology and Geology* (*in Chinese*), **5**(3): 63-74
[7] Guo G A, Feng R. 1992. The joint inversion of 3-D velocity structure and source parameters in Xinfengjiang reservoir. *Chiese Journal of Geophysics*(*in Chinese*),**35**(3): 331-342
[8] Guo G A, Liu T P, Qin N G, et al. 2004．Analysis on small-earthquake composite fault plane solutions from 1961 to 1999 in Xinfengjiang reservoir area. *Acta Seismologica sinica*, **26**(3), 261-268
[9] Gutenberg R, Richter C F. 1994. Frequency of earthquakes in California. *Bull. Seism. Soc. Am*. **34**(4):185-188
[10] Jiangxi Bureau of Geology and mineral resources. 1984. Regional Geology of Jiangxi Province．Beijing：Geological Publishing House．
[11] Kissling E，Ellsworth W L，Eberhard-Phillips D，et al．1994. Initial reference models in local earthquake tomography. *J Geophys Res*, (99):19635-19646
[12] Liu F T. 1984. Simultaneous inversion of earthquake hypocennters and velocity structure(1)—theory and method. *Chinese Journal of Geophysics (in Chinese)*, **27**(2): 167-175
[13] Liu F T, Qu K X, WU H, et al. 1987. Seismic tomography of North China region. *Chinese*

Journal of Geophysics (in Chinese), 29(5):442-449.

[14] Liu F T，Li Q，Wu H, et al. 1989. On the tomographic inverse method used in velocity image reconstruction. *Acta Geophysica Sinica*, **32**(1): 46-61

[15] Long F，Wen X Z and Xu X W. 2006．Empirical relationship between magnitude and rupture length，and rupture area，for seismogenic active faults in North China. *Seismology and Geology*, **28**(4): 511-535

[16] Ma H S, Zhang G M, Zhou L Q, et al. 2008. Simultaneous inversion of small earthquake relocation and velocity structure in Sichuan-Yunnan area. *Seismology*, **28**(2): 29-38

[17] Michael A J．1988. Effects of three-dimensional velocity structure on the seismicity of the 1984 Morgan Hill，California，aftershock sequence. *Bull.Seism. Soc. Amer* , (78):1199-1221

[18] Pan J X, Xiao A Y. 1982. The preliminary study of seismic structures and their characteristic activity in Xinfengjiang reservoir area. *Seismology and Geology* (*in Chinese*), **4**(2): 53-58

[19] Pan S Z, Zhang X K, YangZ X,et al. 2007. Tomographic determination of the upper crustal structure in Jiashi strong earthquake swarm region----joint inversion of explosion and earthquake data.*Chinese Journal of Geophysics (in Chinese)*,50(5):1456~1463

[20] Pavlis L G，Booker J R．1980. The mixed discrete-continuous inverse problem：application to the simultaneous determination of earthquake hypocenters and velocity structure. *J Geophys Res*, (85):4801-4810

[21] Scholz C H. 1968. The frequency-magnitude relation of microfracturing in rock and its relation to earthquakes. *Bull. Seism. Soc. Am*. **58**(1):399-415

[22] Schorlemmer D, Wiemer S, Wyss M. 2005. Variations in earthquake-size distribution across different stress regimes. *Nature*,**437**(7058):539-542

[23] Spencer C，Gubbins D．1983. Travel time inversion for simultaneous earthquake location and velocity structure determination in laterally varying media. *Geophys J R Astron Soc*, **63**(1):95-116

[24] Thurber C H．1983. Earthquake locations and three-dimensional crustal structure in the Coyote late area, Central California. *J Geophys Res*, (88):8226-8236

[25] Urbancic T I, Trifu C I, Long J M, et al. 1992. Space-time correlation of b values with stress release. *Pure Appl. Geophys*. **139**(3-4):449-462

[26] Wang M Y, Yang M Y, Hu Y L, et al. 1976. A preliminary study on the mechanism of the reservoir impounding earthquakes at Hsinfengkiang. *Science in china Ser A* (*in Chinese*), (1): 85-97

[27] Wei B L, Chen P L, Li F G, et al. 1991. Focal mechanisms and tectonic stress field of the Xinfengjiang earthquakes. *Acta Seismologica Sinica* (*in Chinese*),**13**(4)：462-470

[28] Wen Z G, Yang M L, Ye X W, et al. 2005. Shear wave velocity structure in the east region of Guangdong province. *Northwestern Seismological Journal*,**27**(2): 154-157

[29] Wiemer, S., Wyss M. 1997. Mapping the frequency-magnitude distribution in asperities: An improved technique to calculate recurrence times. *J. Geophys. Res*, (102):15115-15128.

[30] Wiemer, S., Benoit J. 1996. Mapping the b-value anomaly at 100 km depth in the Alaska and New Zealand subduction zones. *Geophys. Res. Lett*, **23**: 1557-1560.

[31] Wiemer, S., McNutt S. 1997. Variations in frequency-magnitude distribution with depth in two volcanic areas: Mount St. Helens, Washington, and Mt. Spurr, Alaska. *Geophys. Res. Lett*, **24**: 189-192.

[32] Wiemer, S., McNutt S.R., Wyss M. 1998. Temporal and three-dimensional spatial analysis of the frequency-magnitude distribution near Long Valley caldera, California. *Geophys. J. Int ,* **134**: 409 - 421.

[33] Wiemer, S., Malone, S. 2001. A software package to analyze seismicity: zmap. *Seismological Research Letters*, **27**(2):374-383.

[34] Wyss M, Schorlemmer D and Wiemer S. 2000. Mapping asperities by minima of local

recurrence time: The San Jacinto-Elsinore fault zones, *J. Geophys. Res*, (105): 7829-7844
[35] Wyss M. 1973. Towards a physical understanding of the earthquake frequency distribution. *Geophys. J. Int.,* **31**(4):341-359
[36] Wyss, M., Shimazaki K., Wiemer S. 1997. Mapping active magma chambers by b-values beneath the off-Ito volcano, Japan. *J. Geophys. Res*., (102): 20413-20422 .
[37] Wyss, M., Wiemer S. 2000. Change in the probability for earthquakes in Southern California due to the Landers magnitude 7.3 earthquake. *Science*, **90**(5495): 1334-1338.
[38] Wyss M., Stefansson R. 2006. Nucleation points of recent mainshocks in Southern Iceland, mapped by b-value. *Bull. Seism. Soc. Am*. **96**(2):599-608
[39] Xu H L, Qiu X L, Zhao M H et al. 2005. Characteristics of crustal structure and source structure in the epicentral region of the Nan'ao earthquake (m=7.5) in the northeastern South China Sea. *Chinese Science Bulletin* (*in Chinese*), **51**(Suppl 2)，83-91.
[40] Yi G X, Wen X Z, Fan J, et al. 2004. Assessing current faulting behaviors and seismic risk of the Anninghe-Zemuhe fault zone from seismicity parameters. *Acta seismologica sinica*(*in Chinese*), 26(3):294-303.
[41] Yi G X, Wen X Z, Wang S W, et al. 2006. Study on Fault sliding behaviors and strong-earthquake risk of the Longmenshan-Minshan fault zones from current seismicity parameters. *Earthquake Research in China*(*in Chinese*), 22(2):117-125.
[42] Yi G X, Wen X Z, Xin H, et al. 2013. Stress state and major-earthquake risk on the southern segment of the Longmen Shan fault zone. *Chinese Journal of Geophysics (in Chinese)*, 56(4):1112-1120.
[43] Yao B C，Zeng W J，Hayes D E，et al. 1994. China-Us cooperation Investigation of the south China sea geological report GMSCS. Wuhan: China University of Geosciences Press
[44] Yang Z X, Liu B F, Wang Q C, et al. 2011. 2-D p-wave velocity structure in the Xinfengjiang reservoir area—Results of Yingde-Heyuan—Luhe deep seismic sounding profile. *Progress in Geophysics*（*in Chinese*）, **26**(6): 1968~1976
[45] Ye X W, Huang Y M, Hu X M and Liu J. 2013. Locatioin of the Dongyuan Ms4.8 earthquake sequence of Guangdong and 3D P-wave velocity structure in and around source region. *Acta Seismologica Sinica*, **35**(6): 809-818
[46] Zhao D，Hasegawa A, Horiuchi S．1992. Tomographic imaging of P and S wave velocity structure beneath northeastern Japan. *J Geophys Res*, (97):19909-19928
[47] Zhao M H, Qiu X L, Ye C M, et al. 2004. Analysis on deep crustal structure along the onshore-offshore seismic profile across the Binhai（Littoral）Fault Zone in northeastern South China Sea. *Chinese J, Geophys* (*in Chinese*), 47(5):845~852
[48] Zhao Y Z, Wu Z L. 2008. Mapping the b-values along the Longmenshan fault zone before and after the 12 May 2008, Wenchuan, China, Ms8.0 earthquake. *Nat. Hazards Earth Syst*. Sci. **8**:1375-1385.
[49] Zheng Q S，Zhu J S，Cao J M，et al. 2004. The data processing of lithospheric crust in velocity structure in South China. *Computing Techniques for Geophysical and Geochemical Exploration*, 26(2): 97-100
[50] Zheng Q S，Zhu J S，Xuan R Q，et al．2003. An approach to the crustal velocities in southern China. *Sedimentary Geology and Tethyan Geology*, **23**(12): 9-13
[51] Zhou L Q, Liu F T, Chen X F. 2006. Simultaneous tomography of 3_D velocity structure and interface.*Chinese J.Geophys. (in Chinese)*, 49(4):1062~1067
[52] Zhou L Q，Liu J，Ma H S，et al．2009，Simultaneous inversion for the 2003 Dayao M6.2 and M6.1 earthquakes sequence locations and velocity structure in the hypocentral area. *Earthquake,* **29**(2)：12-24
[53] Zhou L Q，Liu J and Zhang X D．2007．Evolution of 3D velocity structure before DaYao M6.2 and M6.1 earthquakes in2003. *Acta Seismologica Sinica*, 29(1): 20~30